

## Research Article

# Dihydroartemisinin Promoted Bone Marrow Mesenchymal Stem Cell Homing and Suppressed Inflammation and Oxidative Stress against Prostate Injury in Chronic Bacterial Prostatitis Mice Model

Shen Li <sup>1</sup>, Yongzhang Li <sup>2</sup>, Xiaozhe Su <sup>1</sup>, Aiyun Han <sup>1</sup>, Yang Cui <sup>1</sup>, Shuyue Lv <sup>1</sup>, Jin Zhang <sup>1</sup>, and Chao Li <sup>1</sup>

<sup>1</sup>Department of Urology, Shijiazhuang City People's Hospital, Shijiazhuang 050000, Hebei, China

<sup>2</sup>Department of Urology, Hebei Province of Chinese Medicine, Shijiazhuang 050011, Hebei, China

Correspondence should be addressed to Shen Li; 19803311531@139.com

Received 13 July 2021; Accepted 8 November 2021; Published 15 December 2021

Academic Editor: Sergio R. Ambrosio

Copyright © 2021 Shen Li et al. This is an open access article distributed under the Creative Commons Attribution License, which permits unrestricted use, distribution, and reproduction in any medium, provided the original work is properly cited.

Although bone marrow mesenchymal stem cells (BMMSCs) are effective in treating chronic bacterial prostatitis (CBP), the homing of BMMSCs seems to require ultrasound induction. Dihydroartemisinin (DHA) is an important derivative of artemisinin (ART) and has been previously reported to alleviate inflammation and autoimmune diseases. But the effect of DHA on chronic prostatitis (CP) is still unclear. This study aims to clarify the efficacy and mechanism of DHA in the treatment of CBP and its effect on the accumulation of BMMSCs. The experimental CBP was produced in C57BL/6 male mice via intraurethraly administered *E. coli* solution. Results showed that DHA treatment concentration-dependently promoted the accumulation of BMMSCs in prostate tissue of CBP mice. In addition, DHA and BMMSCs cotreatment significantly alleviated inflammation and improved prostate damage by decreasing the expression of proinflammatory factors such as TNF- $\alpha$ , IL-1 $\beta$ , and chemokines CXCL2, CXCL9, CXCL10, and CXCL11 in prostate tissue of CBP mice. Moreover, DHA and BMMSCs cotreatment displayed antioxidation property by increasing the production of glutathione peroxidase (GSH-Px), SOD, and decreasing malondialdehyde (MDA) expression. Mechanically, DHA and BMMSCs cotreatment significantly inhibited the expression of TGF $\beta$ -RI, TGF $\beta$ -RII, phosphor (p)-Smad2/3, and Smad4 in a dose-dependent manner while stimulated Smad7 expression in the same manner. In conclusion, our findings provided evidence that DHA effectively eliminated inflammatory and oxidative stress against prostate injury, and this effect involved the TGF- $\beta$ /Smad signaling pathway in CBP.

## 1. Introduction

Chronic prostatitis (CP) is a common disease in the urology clinic. The clinical manifestations of CP include abnormal urination, pain, and sexual dysfunction, especially symptoms of voiding dysfunction [1]. Based on symptomatology, and the presence or absence of leukocytes in semen and prostatic fluid, CP was classified into three categories, namely, chronic bacterial prostatitis (CBP), chronic non-bacterial prostatitis (CNP), and experimental autoimmune prostatitis (EAP) [1]. The traditional treatment of CP was mainly antibiotics,  $\alpha$ -blockers, and anti-inflammatory drugs,

combined with psychological and physical therapies [2]. However, the treatment effects of these methods are not very satisfactory. Due to the multitargeted therapy and fewer side effects of traditional Chinese medicines (TCMs), there are more and more research studies that have focused on the prevention and treatment of CP with TCM [3]. Many TCM compound preparations and their active components such as *Abacopteris penangiana* [4], Bazhengsan [5], and flavonoids [6] were effective in the treatment of CP.

Artemisinin (ART) was a well-known clinically important antimalarial drug, which was extracted from *Artemisia annual leaves* and was first discovered and reported by

Professor Tu Youyou, an outstanding pharmacologist in China [7]. Dihydroartemisinin (DHA,  $C_{15}H_{24}O_5$ ) is a sesquiterpenoid compound and is an important derivative of ART. As DHA research progresses, the pharmacological benefits of DHA were not only limited to the treatment of malaria but also showed great promise in anti-inflammatory and immune regulation. Previous studies have found that DHA was effective in the treatment of inflammatory diseases and oxidative stress, especially for acute kidney injury [8], pulmonary fibrosis [9], and airway inflammation [10]. It is preliminarily confirmed that DHA could inhibit inflammatory bowel disease (IBD) by regulating the balance of Th17/Treg cells [11]. Furthermore, more and more evidence showed that DHA also had powerful neuroprotective [12], antitumor [13, 14], and inhibiting angiogenic effects [15]. DHA was widely reported inhibiting the progression of prostate cancer [16, 17]. The occurrence of prostate cancer and prostatitis was closely related [18]. However, the function and potential molecular mechanism of DHA on prostatitis are unclear.

Bone marrow mesenchymal stem cells (BMMSCs) are a stem cell population with rapid population proliferation, multidirectional differentiation, low immunogenicity, immune suppression, and tissue repair ability [19]. BMMSCs have been applied in clinical inflammatory disease treatment. Intriguingly, the previous research in CBP rats found that microbubble-mediated ultrasound-induced BMMSC accumulation inhibited inflammation and decreased TNF- $\alpha$  and IL-1 $\beta$  expressions [20]. In this study, we aimed to investigate the role of DHA treatment and its involvement in BMMSC homing in a mouse model of CBP.

## 2. Methods and Materials

**2.1. Reagents.** DHA was purchased from KPC Pharmaceuticals, Inc. (Chongqing, China). Product batch number: C00220160402.

**2.2. Animals.** C57BL/6 male mice (SPF grade, 9–11 weeks) were purchased from Dashuo Animal Experiment Co., Ltd. (Chengdu, Sichuan; license number: SCXY (Chuan) 2020–034). The feeding environment was  $25 \pm 1^\circ\text{C}$ , relative humidity 50%–60%, and light/darkness for 12-h circulation. The mice are allowed to freely eat and drink.

**2.3. Animal Grouping and Treatment.** The experimental protocol for the care and use of laboratory animals was approved by the Experimental Animal Ethics Committee of Shijiazhuang City People's Hospital (2021097). The mice were randomly divided into 5 groups ( $n=6$ ), namely, the control group, model group, BMMSCs group, low-dose DHA + BMMSCs group, and high-dose DHA + BMMSCs group. All mice were anesthetized with 1% sodium pentobarbital (50 mg/kg, Merck, Germany) prior to treatment. For the control group, the male mice were instilled with 200  $\mu\text{l}$  phosphate buffer saline (PBS); for the model group, the mice were intraurethraly administered with 200  $\mu\text{l}$  of *E. coli* solution ( $2 \times 10^6$  cfu/ml). After modeling, all mice were

normally fed for 4 weeks. Then, for the BMMSC group, the mice were injected with 30  $\mu\text{l}$  of PBS buffer containing  $1 \times 10^7$  GFP-BMMSCs in the tail vein; for DHA low- and high-dose groups, the mice were given DHA 10 mg/kg/d and 20 mg/kg/d by gavage, respectively. The control and model groups were given 0.9 g/L saline 3 ml/d by gavage. All mice were raised in an SPF environment for another 2 weeks. Finally, the mice were anesthetized with 1% sodium pentobarbital (50 mg/kg) and then euthanized. The prostate tissue was removed for subsequent analysis.

**2.4. Cell Culture.** Mouse BMMSCs were purchased from Procell (#CP-M131, Wuhan, China). The cells were maintained in DMEM/F-12 medium supplemented with 10% fetal bovine prostate tissue (FBS; Gibco, Grand Island, NY) at  $37^\circ\text{C}$  with 5%  $\text{CO}_2$  in a humidified incubator. Then, BMMSCs ( $3 \times 10^3$ /well) were seeded in a 96-well plate and cultured in an incubator ( $37^\circ\text{C}$ , 5%  $\text{CO}_2$ ) for 24 h. Subsequently, 100  $\mu\text{l}$  diluent of GFP-LUC adenovirus ( $1 \times 10^9$  cfu/ml) was transfected into BMMSCs and cultured for 24 h. A fluorescence microscope was used to observe the expression of fluorescence and determine the transfection efficiency.

**2.5. CCK-8 Assay.** The cell viability of GFP-BMMSCs was measured using the Cell Counting Kit-8 (CCK-8, Thermo Fisher Scientific) according to the instructions of the manufacturer. Absorbance was recorded at 450 nm.

**2.6. Hematoxylin and Eosin (H&E) Stain.** Mice prostate tissues were fixed in 4% paraformaldehyde for 24 h and embedded in paraffin to a histopathological study by H&E stain. In brief, each mice prostate paraffin section was deparaffinized and dehydrated with xylene and graded ethanol. After staining with hematoxylin and eosin, the paraffin sections were washed with distilled water and dehydrated with graded ethanol and xylene. The inflammation degree of each prostate tissue was evaluated using a light microscope under 5 random fields.

**2.7. Western Blot Analysis.** Prostate tissues were homogenized using a homogenizer with magnetic beads. Total protein was manufactured using RIPA buffer (Cell Signaling Technology, Inc.). The concentration of protein was determined by a BCA kit (Sigma-Aldrich; Merck KGaA, Germany). Total protein (30  $\mu\text{g}$ /sample) was separated via 10% SDS-PAGE. And then, the separated proteins were transferred to nitrocellulose membranes. The membranes were blocked with 5% nonfat dried milk overnight at  $4^\circ\text{C}$  and incubated with the following corresponding protein antibodies: TGF $\beta$ -RI (1:1000, Abcam, #31013), TGF $\beta$ -RII (1:1000, Abcam, #186838), phosphor (p)-Smad2/3 (1:800, Abcam, #254407), Smad4 (1:1000, CST, #38454), Smad7 (1:1000, Santa Cruz, #365846), and  $\beta$ -actin (1/1000, Boster, #BM0627). Then, the membranes were washed with Tris-buffered saline/0.1% Tween (TBST) and incubated for 1.5 hours with HRP goat anti-rabbit IgG (1:2000, Abcam, #6721). The bands were visualized using the ECL system

(Affinity Biosciences, Cincinnati, Ohio, USA), and  $\beta$ -actin was used as an internal control. The net optical density was measured using Quantity One software (Bio-Rad).

**2.8. Immunofluorescence (IF) Stain.** IF stain was used to determine the expression of CD29, CD44, and CD45 in mouse prostate tissue. Mouse prostate paraffin sections (8  $\mu$ m) were fixed in acetone for 10 min and rinsed 3 times with PBS. Then, the tissue sections were, respectively, incubated at 4°C overnight with rabbit anti-mouse CD29, CD44, and CD45 monoclonal antibodies (1:100, Bioss Biotechnology Ltd., Beijing, China). Sections were rinsed with PBS and incubated with bovine anti-rabbit IgG-FITC (Santa Cruz, USA) for 30 min at room temperature. Finally, sections were incubated with DAPI and observed with a fluorescent microscope.

**2.9. Enzyme-Linked Immunosorbent Assay (ELISA).** The contents of TNF- $\alpha$ , IL-1 $\beta$ , CXCL2, CXCL9, CXCL10, CXCL11, MDA, SOD, and GSH-Px in prostate tissue of CBP mice were measured with ELISA kits (Takara, Tokyo, Japan) following the instructions of the manufacturer. The absorbance measured at 450 nm wavelength was estimated using an enzyme-linked immune monitor (Thermo Fisher Scientific, Inc., USA). The concentrations of TNF- $\alpha$ , IL-1 $\beta$ , CXCL2, CXCL9, CXCL10, CXCL11, MDA, SOD, and GSH-Px in the sample were calculated from the standard curve.

**2.10. Statistical Analysis.** The data were represented as mean  $\pm$  standard deviation. Statistical analysis was performed using SPSS 20.0 (IBM Corp.). One-way analysis of variance (ANOVA) with Tukey's post hoc test of means was used for multiple group comparisons. For comparisons between two groups, Student's unpaired *t*-test was used to assess statistical significance. Differences with a *P* < 0.05 were considered to indicate statistical significance.

### 3. Results

**3.1. Observation of GFP-LUC Adenovirus-Transfected BMSC Viability.** As shown in Figure 1, the green fluorescence was observed in BMSCs after 48 h and 72 h of GFP-LUC adenovirus transfection, which did not affect the viability of BMSCs. Thus, the GFP-labeled BMSCs were then injected into the tail vein for the treatment of CBP mice.

**3.2. DHA Promoted Homing of BMSCs to Prostate Tissue.** As shown in Figures 2(a) and 2(b), compared with the control group and BMSC alone injection group, DHA dose-dependently promoted the aggregation of BMSCs into prostate tissue, as evidenced by increased levels of green fluorescence in prostate tissue. MSCs were able to positively express CD29 and CD44 whereas negatively for CD45. Our IF stain results showed that CD29 and CD44 protein levels were higher in prostate tissue of DHA administration mice than in the control group and BMSC alone injection group (Figures 2(c)–2(e)). However, there was no CD45 expression

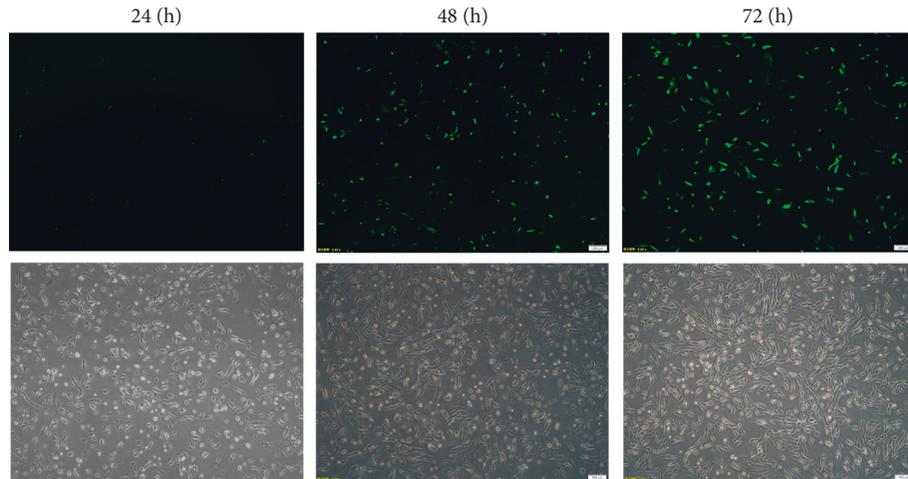
in each group (Figure 2(c)). These data reflected that DHA obviously promoted homing of BMSCs to prostate tissue in CBP mice.

**3.3. Effect of DHA and BMSC Cotreatment on Histopathological Features and Inflammatory Mediators in CBP Mice.** Next, we analyzed the pathological injury of mice prostate tissue. Histological analysis showed that in the control group, the glandular cavity epithelial cell layer had a complete structure and was arranged in a columnar shape (Figure 3(a)). There was no fibrous tissue hyperplasia and infiltrating inflammatory cells in the interstitium (Figure 3(a)). Both the CBP group and the CBP + BMSC group showed the necrosis of epithelial cells. A large number of lymphocytes and plasma cells were infiltrated in the interstitium (Figure 3(a)). Low-dose and high-dose DHA significantly improved the pathological damage of prostate tissue in a concentration-dependent fashion (Figure 3(a)). Furthermore, ELISA analysis revealed upregulation of TNF- $\alpha$  and IL-1 $\beta$  in prostate tissue of CBP mice, which was inhibited by cotreatment of DHA and BMSCs (Figure 3(b)).

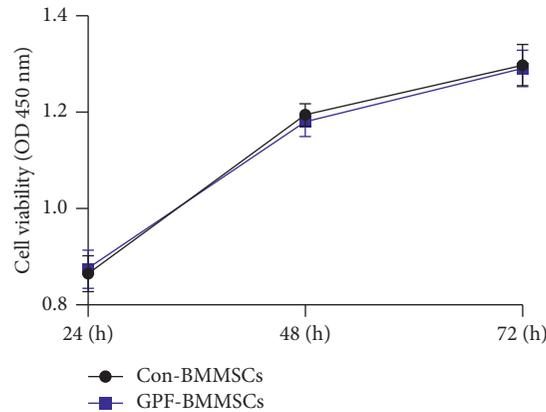
The chemokines of the CXC family were reported to produce obvious proinflammatory effects in a series of diseases, especially participated in the formation and development of benign prostate hyperplasia (BPH) and prostate cancer [21]. Thus, we also detected the expression levels of chemokines in prostate tissue of CBP mice by ELISA assay. The secretions of CXCL2, CXCL9, CXCL10, and CXCL11 chemokines were increased in the model group and BMSC alone treatment group, which were blocked by low/high-dose DHA and BMSC cotreatment (Figures 3(c)–3(f)).

**3.4. DHA and BMSCs Cotreatment Attenuated Oxidative Stress in CBP Mice.** Several clinical studies demonstrated oxidative stress played an essential role in the progression of CP [22–24]. To confirm that the cotreatment of DHA and BMSCs can also improve oxidative stress in CBP mice, we tested MDA, SOD, and GSH-Px levels in prostate tissue of CBP mice using ELISA kits. A statistically significant increase in the model group was documented in terms of MDA activity (Figure 4(a)). Decreased SOD and GSH-Px activities were also found in the model group and BMSC alone treatment group (Figures 4(b) and 4(c)). Furthermore, compared with those in the BMSC alone treatment group, the SOD and GSH-Px activities were increased in the low-dose DHA + BMSC group and high-dose DHA + BMSC group, while the MDA level was decreased (Figures 4(a) and 3(c)).

**3.5. DHA and BMSC Cotreatment Inhibited TGF- $\beta$ /Smad Signaling Pathway in CBP Mice.** Finally, we preliminarily investigated the mechanism of improvement of DHA in mice with prostatitis. The results indicated that in prostate tissue of CBP mice and BMSC alone-treated mice, the expression of TGF $\beta$ -RI, TGF $\beta$ -RII, p-Smad2/3, and Smad4 was markedly increased (Figures 5(a)–5(e)). After low-dose

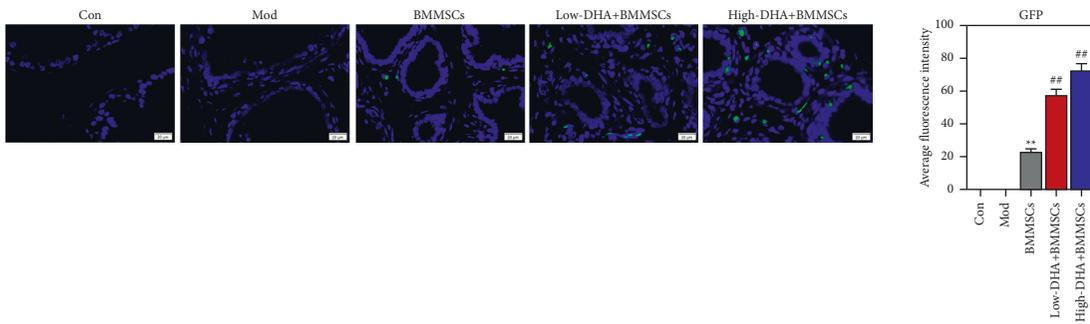


(a)



(b)

FIGURE 1: Observation of GFP-LUC adenovirus-transfected BMSC viability. (a) Green fluorescent levels in BMMSCs at 24 h 48 h and 72 h after transfection with GFP-LUC adenovirus ( $\times 100$  magnification). The scale bar indicates  $200 \mu\text{m}$ . (b) Cell viability was tested using the CCK-8 assay. For B mean  $\pm$  standard errors of means are reported.



(a)

(b)

FIGURE 2: Continued.

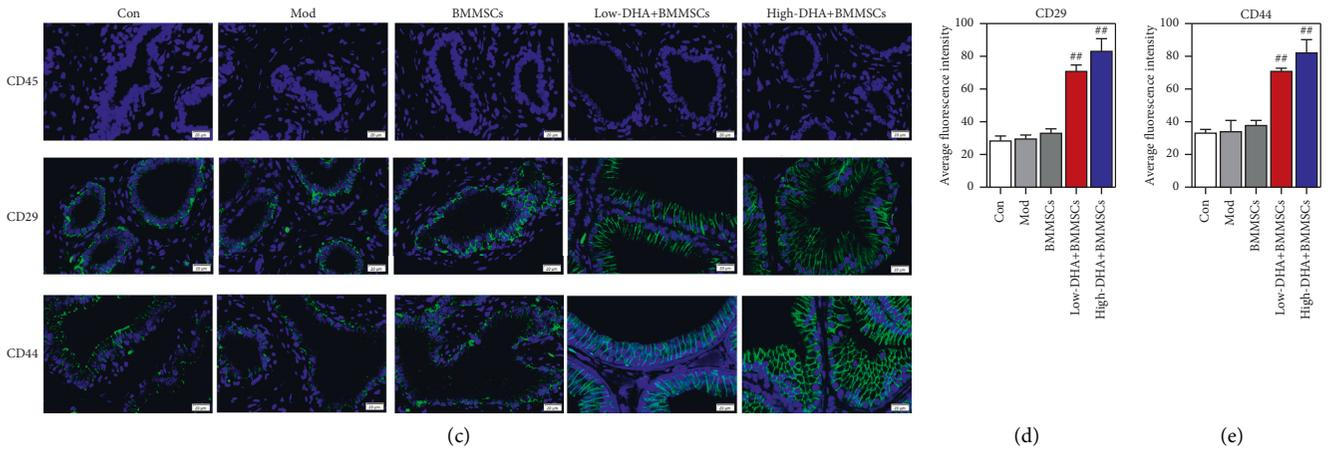


FIGURE 2: DHA promoted homing of BMMSCs to prostate tissue. (a) Fluorescence images showing GFP+ cells in prostate tissue ( $\times 200$  magnification). (b) Average fluorescence intensity of GFP. (c-e) Fluorescence images and average fluorescence intensity of CD45, CD29, and CD44 levels in prostate tissue ( $\times 200$  magnification). The scale bar indicates  $20 \mu\text{m}$ . \*\*denotes  $P < 0.01$  vs con group and ##denotes  $P < 0.01$  vs BMMSCs group. For B, D, and E, mean  $\pm$  standard errors of means are reported.

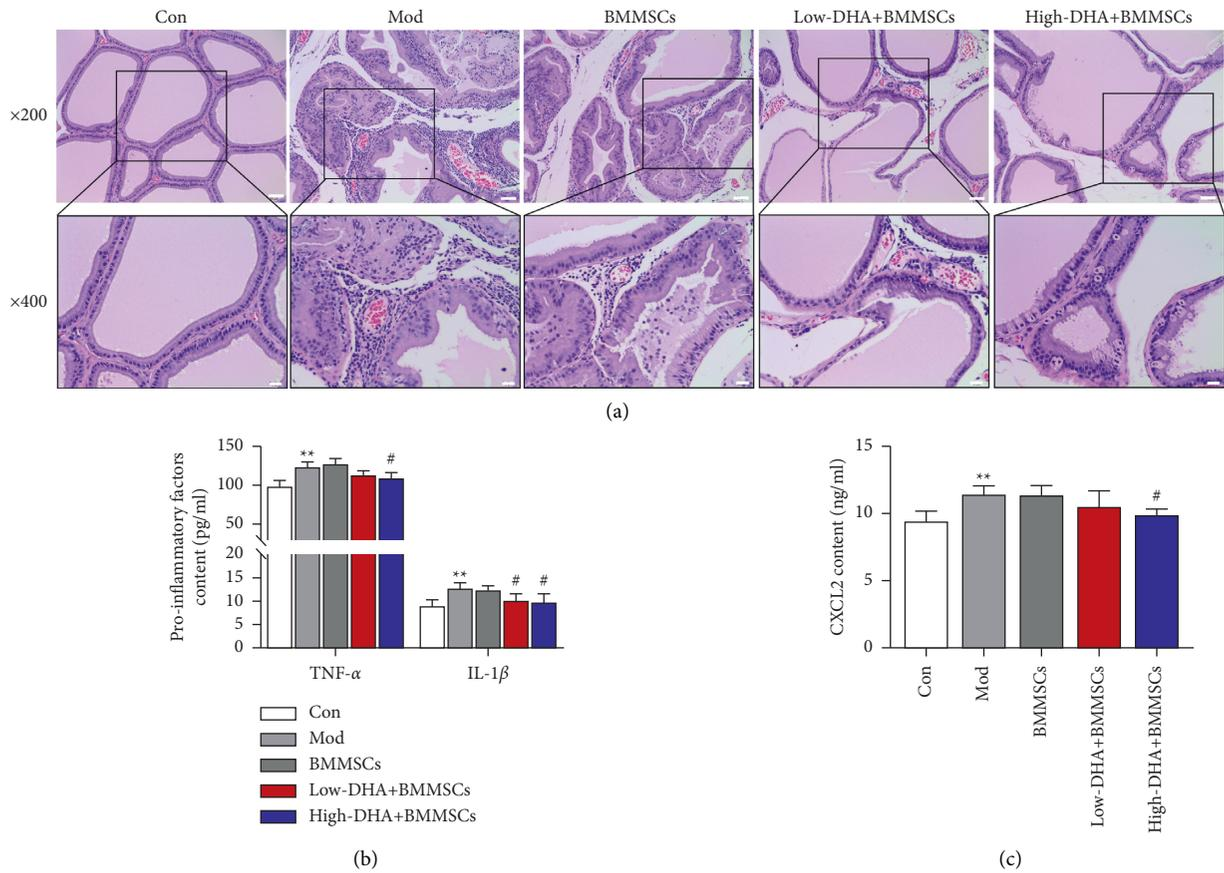


FIGURE 3: Continued.

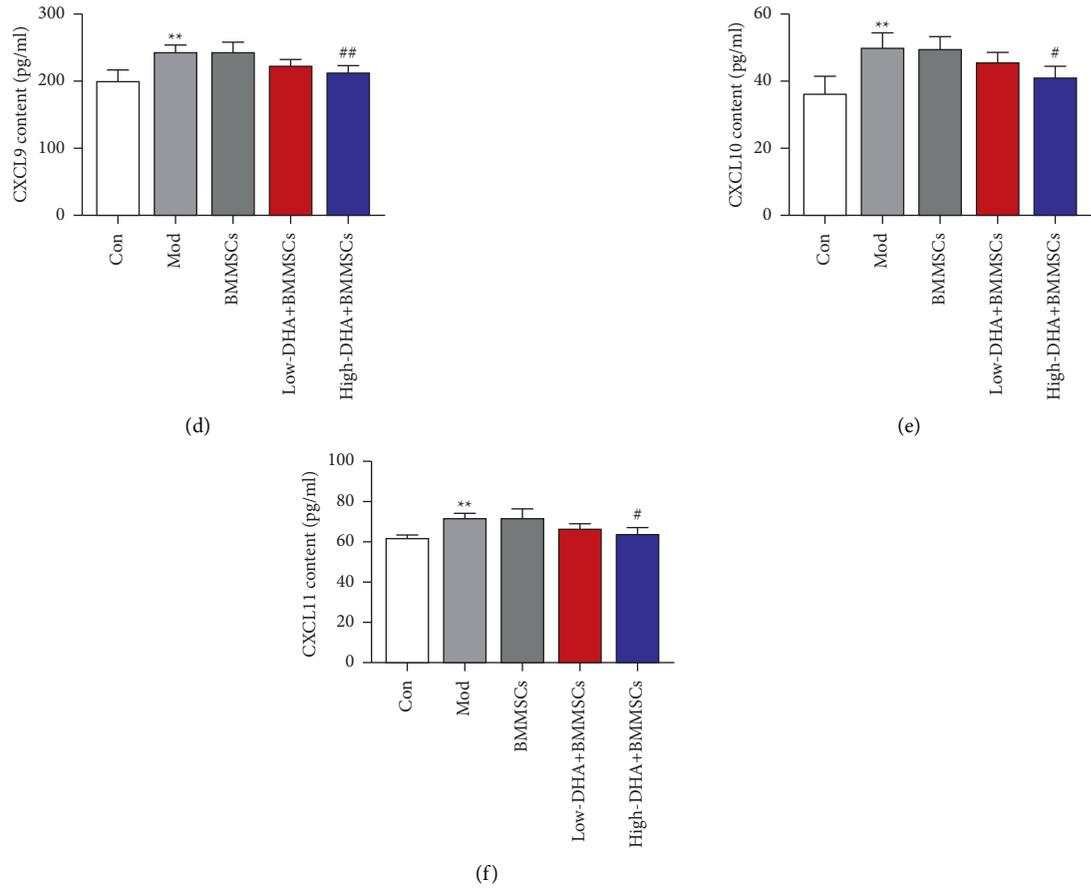


FIGURE 3: Effect of DHA and BMMSC cotreatment on histopathological features and inflammatory mediators in CBP mice. (a) H&E stain of prostate tissue from C57BL/6 mice in the different groups. The scale bar indicates 50  $\mu\text{m}$  ( $\times 200$  magnification) and 20  $\mu\text{m}$  ( $\times 400$  magnification). (b–f) Quantifications of TNF- $\alpha$ , IL-1 $\beta$ , CXCL2, CXCL9, CXCL10, and CXCL11 levels in prostate tissue of all groups were examined using an ELISA assay. \*\*denotes  $P < 0.01$  vs con group, # denotes  $P < 0.05$  vs BMMSCs group, and ## denotes  $P < 0.01$  vs BMMSCs group. For (b)–(f), mean  $\pm$  standard errors of means are reported.

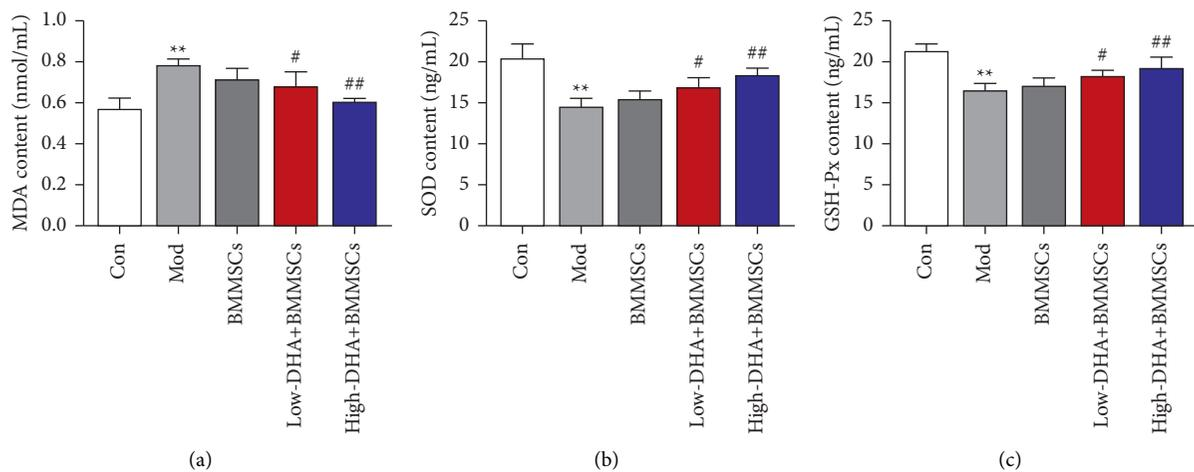


FIGURE 4: DHA and BMMSC cotreatment attenuated the oxidative stress in CBP mice. Expression of oxidative stress-related factors MDA (a), SOD (b), and GSH-Px (c) in the prostatic tissues of mice was detected by ELISA. \*\*denotes  $P < 0.01$  vs con group, # denotes  $P < 0.05$  vs BMMSCs group, and ## denotes  $P < 0.01$  vs BMMSCs group. For all the graphs, mean  $\pm$  standard errors of means are reported.

and high-dose DHA cotreatment with BMMSCs, all elevated levels of these core proteins in the TGF- $\beta$ /Smad signaling pathway were reversed in prostate tissue (Figures 5(a)–5(e)).

In addition, DHA and BMMSC cotreatment dose-dependently suppressed the downregulation of Smad7 induced by prostatitis (Figures 5(a) and 5(f)).

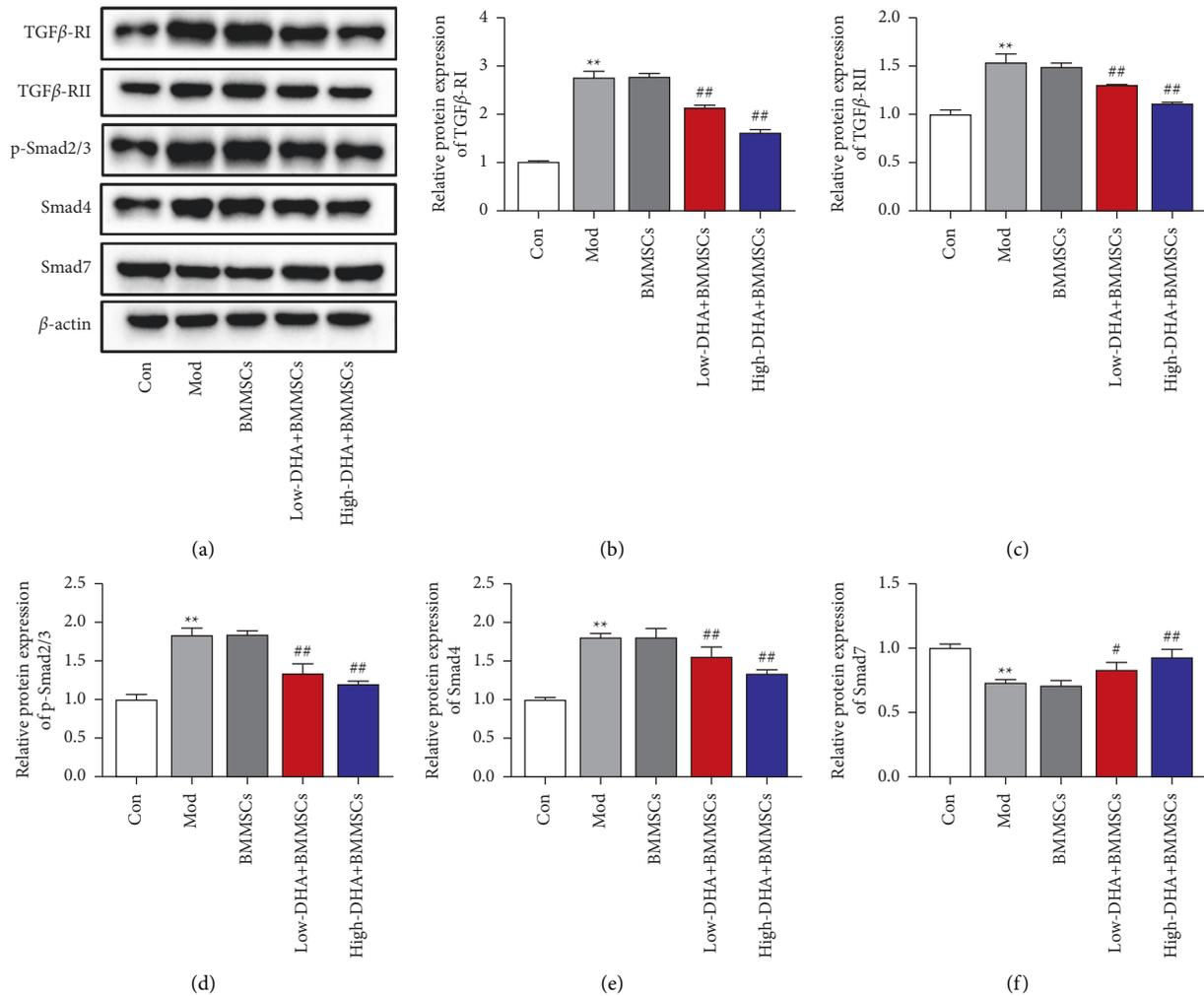


FIGURE 5: DHA inhibited TGF- $\beta$ /Smad signaling pathway in CBP mice. (a) Representative bands of Western blot analysis. Expression of TGF $\beta$ -R1 (b), TGF $\beta$ -R2 (c), p-Smad2/3 (d), Smad4 (e), and Smad7 (f) in the prostatic tissues of mice was detected by Western blot. \*\*denotes  $P < 0.01$  vs con group, # denotes  $P < 0.05$  vs BMMSCs group, and ## denotes  $P < 0.01$  vs BMMSCs group. For (b)–(f), mean  $\pm$  standard errors of means are reported.

#### 4. Discussion

In this study, the results of significant accumulation of BMMSCs observed in the prostate tissue of the DHA group confirmed a possible link between DHA treatment and BMMSC homing. Furthermore, our results evaluated the effect of DHA and BMMSC cotreatment on oxidative stress and inflammation in CBP mice.

Earlier studies showed that mesenchymal stem cells (MSCs) played the role of inhibiting the inflammatory response through inhibiting T cell, B cell, and antigens that presented cell proliferation and suppressing proinflammatory factor generation [25]. MSC concentration-dependently inhibited the secretion of TNF- $\alpha$  and IL-12 from dendritic cells and promoted anti-inflammatory factor IL-10 expression [26]. Meanwhile, MSCs induced division arrest T cells in G0/G1 phase and inhibited Th1-cell proliferation [27]. In addition, TNF- $\alpha$  and IL-12 stimulated MSCs to secrete T-cell chemokines such as CXCL9, CXCL10, and CXCL11, which further promoted T-cell

aggregation toward MSCs, thereby fully exerting immunoregulatory capacity [28]. Moreover, BMMSCs had excellent treatment effects on inflammatory disease. In a rat model of bronchial asthma, intravenously injected BMMSCs specifically accumulated in the lung inflammation after 1 hour. Subsequently, BMMSCs reduced the levels of Th2 cell-related inflammatory factor levels in bronchial lavage fluid and IgG1 and IgE levels in serum, thereby reducing the inflammatory response [29]. In the treatment of *E. coli* pneumonia, MSCs could reduce bacterial growth in the bronchoalveolar lavage (BAL) fluid and pulmonary inflammatory response by secreting antibacterial peptide hCAP-18/LL-37 [30]. However, our results indicated that BMMSC alone treatment did not seem to exert a favorable anti-inflammatory effect in the CBP model. This may be due to the blood-prostate barrier preventing the efficient accumulation of BMMSCs into the prostate tissue [31]. Importantly, in our CBP model, we discovered that DHA treatment promoted the accumulation of BMMSCs into the prostate tissue in a concentration-dependent manner. Hence, we deduced that DHA

treatment, accompanied by BMMSCs homing, was likely to play a role in improving CBP injury.

We then investigated the effect of cotreatment with DHA and BMMSCs on inflammation in CBP mice. This study demonstrated that high-dose DHA and BMMSC cotreatment markedly diminished inflammation in prostate tissue of CBP mice, which was manifested as decreases in the expression levels of proinflammatory factor TNF- $\alpha$ , IL-1 $\beta$ , and chemokines CXCL2, CXCL9, CXCL10, and CXCL11. TNF- $\alpha$  is an important proinflammatory cytokine secreted by mononuclear macrophages, neutrophils, and T cells [32]. IL-1 $\beta$  promoted the release of protein hydrolases from neutrophils and activated T cells to accumulate in the prostate tissue, finally causing an immune response [33]. The study found that TNF- $\alpha$  and IL-1 $\beta$  levels were significantly higher in prostatic secretions of patients with CP [34]. Moreover, increased levels of chemokines have been described in clinical samples from chronic prostatitis/chronic pelvic pain syndrome (CP/CPPS) patients [35]. DHA was previously reported to hinder the production of proinflammatory cytokines IL-1 $\beta$ , TNF- $\alpha$ , and IL-6 via regulating NF- $\kappa$ B signaling in acute lung injury (ALI) [36]. Moreover, DHA also exerted an anti-inflammatory effect through the deactivation of NLRP3 inflammasome and p38 MAPK signaling [37]. DC32, a dihydroartemisinin derivative, was found to significantly inhibit the transcription of chemokines (CXCL12 and CX3CL1) and IL-6 in rheumatoid arthritis (RA) [38]. These studies were consistent with our results showing the excellent anti-inflammatory effect of DHA and BMMSC cotreatment.

Studies have shown that the development of CP was also closely related to oxidative stress [39, 40]. CBP patients produced excessive amounts of ROS in plasma that disrupted the intracellular environment and formed toxic products such as lipid peroxide MDA [24]. SOD participated in the metabolism of reactive oxygen species, and GSH-Px inhibited the accumulation of lipid peroxidation, both of which protected cells from oxidative damage. It was found that in CP/CPPS model rats, lycopene treatment upregulated GSH-Px and SOD levels and downregulated MDA content [41]. In this study, as observed through ELISA assays, DHA and BMMSC cotreatment also significantly eliminated oxidative stress in CBP mice that suppressed the production of MDA level and promoted the levels of SOD and GSH-Px in prostate tissue. Therefore, SOD, MDA, and GSH-Px indirectly reflect the oxidation resistance of DHA and BMMSC cotreatment in CBP. Similarly, previous studies explained that DHA treatment significantly decreased oxidative damage to attenuate lung injury [42] and kidney injury [8].

Previous reports have suggested that TGF- $\beta$ /Smad signaling played critical roles during inflammation and oxidative stress [43, 44]. Of the signaling cascade, the heterotrimer formed by TGF- $\beta$ , TGF $\beta$ -RI, and TGF $\beta$ -RII phosphorylated Smad2/3 proteins and ultimately initiated transcription of the relevant target gene with the cooperation of Smad4 [45]. On the other hand, the combination of Smad7 and TGF- $\beta$ RI could hinder the activation of Smad2/3 and control TGF- $\beta$  signaling in a negative feedback manner [45]. TGF- $\beta$ /Smad signaling pathway has been long

considered as a key mediator in the suppression of inflammation, such as in renal inflammation [46] and rheumatoid arthritis [47]. However, pinocembrin-inhibited TGF- $\beta$ /Smad signaling ameliorated oxidative stress and inflammation in a liver fibrosis model [44]. We found that DHA and BMMSC cotreatment inhibited the activation of the TGF- $\beta$ /Smad signaling pathway in prostate tissue of CBP mice. These opposite results may be due to the interaction of TGF- $\beta$ /Smad with other cytokine signaling in the inhibition and promotion of inflammation [43].

In conclusion, DHA performed potent anti-inflammatory and antioxidant effects in CBP mice by promoting the accumulation of BMMSCs into the prostate tissue. Meanwhile, the homing of BMMSCs promoted by DHA inhibited the activation TGF- $\beta$ 1/Smad signaling pathway. The combination therapy of DHA and BMMSCs has shown excellent promise in the treatment of CP.

## Data Availability

The datasets used or analyzed during the current study are available from the corresponding author on reasonable request.

## Conflicts of Interest

The authors declare that they have no competing interests.

## Acknowledgments

This study was supported by a grant from the Scientific Research Project of Hebei Health Commission (nos: 20181118 and 20210302), the Scientific Research Project of Hebei Provincial Administration of Traditional Chinese Medicine (no: 2020013), and the Scientific Research Project of Hebei College of Traditional Chinese Medicine (no: KTY2019015).

## References

- [1] J. D. Holt, W. A. Garrett, T. K. McCurry, and J. M. Teichman, "Common questions about chronic prostatitis," *American Family Physician*, vol. 93, pp. 290–296, 2016.
- [2] A. Thakkinstian, J. Attia, T. Anothaisintawee, and J. C. Nickel, " $\alpha$ -blockers, antibiotics and anti-inflammatories have a role in the management of chronic prostatitis/chronic pelvic pain syndrome," *BJU International*, vol. 110, no. 7, pp. 1014–1022, 2012.
- [3] Y. Xue, Y. Duan, X. Gong, W. Zheng, and Y. Li, "Traditional Chinese medicine on treating chronic prostatitis/chronic pelvic pain syndrome," *Medicine*, vol. 98, no. 26, Article ID e16136, 2019.
- [4] X. Yang, L. Yuan, J. Chen, C. Xiong, and J. Ruan, "Multi-targeted protective effect of Abacopteris penangiana against carrageenan-induced chronic prostatitis in rats," *Journal of Ethnopharmacology*, vol. 151, no. 1, pp. 343–351, 2014.
- [5] Y. Xiong, X. Qiu, W. Shi, H. Yu, and X. Zhang, "Anti-inflammatory and antioxidant effect of modified Bazhengsan in a rat model of chronic bacterial prostatitis," *Journal of Ethnopharmacology*, vol. 198, pp. 73–80, 2017.



- [6] J. Chen, H. Song, J. Ruan, and Y. Lei, "Prostatic protective nature of the flavonoid-rich fraction from *Cyclosorus acuminatus* on carrageenan-induced non-bacterial prostatitis in rat," *Pharmaceutical Biology*, vol. 52, pp. 491–497, 2013.
- [7] Y. Tu, "Artemisinin-A gift from traditional Chinese medicine to the world (nobel lecture)," *Angewandte Chemie International Edition*, vol. 55, no. 35, pp. 10210–10226, 2016.
- [8] X. Liu, J. Lu, Y. Liao et al., "Dihydroartemisinin attenuates lipopolysaccharide-induced acute kidney injury by inhibiting inflammation and oxidative stress," *Biomedicine & Pharmacotherapy*, vol. 117, Article ID 109070, 2019.
- [9] D. Yang, W. Yuan, C. Lv et al., "Dihydroartemisinin suppresses inflammation and fibrosis in bleomycin-induced pulmonary fibrosis in rats," *International Journal of Clinical and Experimental Pathology*, vol. 8, pp. 1270–1281, 2015.
- [10] M. Wei, X. Xie, X. Chu, X. Yang, M. Guan, and D. Wang, "Dihydroartemisinin suppresses ovalbumin-induced airway inflammation in a mouse allergic asthma model," *Immunopharmacology and Immunotoxicology*, vol. 35, no. 3, pp. 382–389, 2013.
- [11] S. C. Yan, Y. J. Wang, Y. J. Li et al., "Dihydroartemisinin regulates the Th/treg balance by inducing activated CD4+ T cell apoptosis via heme oxygenase-1 induction in mouse models of inflammatory bowel disease," *Molecules*, vol. 24, p. 2475, 2019.
- [12] Y. Zhao, Z. Long, Y. Ding et al., "Dihydroartemisinin ameliorates learning and memory in Alzheimer's disease through promoting autophagosome-lysosome fusion and autolysosomal degradation for  $\alpha\beta$  clearance," *Frontiers in Aging Neuroscience*, vol. 12, p. 47, 2020.
- [13] C. Qu, J. Ma, X. Liu et al., "Dihydroartemisinin exerts anti-tumor activity by inducing mitochondrion and endoplasmic reticulum apoptosis and autophagic cell death in human glioblastoma cells," *Frontiers in Cellular Neuroscience*, vol. 11, p. 310, 2017.
- [14] R. Yu, L. Jin, F. Li et al., "Dihydroartemisinin inhibits melanoma by regulating CTL/Treg anti-tumor immunity and STAT3-mediated apoptosis via IL-10 dependent manner," *Journal of Dermatological Science*, vol. 99, no. 3, pp. 193–202, 2020.
- [15] L. Ma, X. Zhao, Y. Liu, J. Wu, X. Yang, and Q. Jin, "Dihydroartemisinin attenuates osteoarthritis by inhibiting abnormal bone remodeling and angiogenesis in subchondral bone," *International Journal of Molecular Medicine*, vol. 47, p. 22, 2021.
- [16] J. D. Pancez, K. Duncan, D. Sekar et al., "Dihydroartemisinin inhibits prostate cancer via JARID2/miR-7/miR-34a-dependent downregulation of Axl," *Oncogenesis*, vol. 8, no. 3, p. 14, 2019.
- [17] J. Kong, S.S. Li, Q. Ma, L. Liu, and J. Zheng, "Effects of dihydroartemisinin on HSP70 expression in human prostate cancer PC-3 cells," *Andrologia*, vol. 51, no. 6, Article ID e13280, 2019.
- [18] Y. Liu, R. Mikrani, D. Xie et al., "Chronic prostatitis/chronic pelvic pain syndrome and prostate cancer: study of immune cells and cytokines," *Fundamental & Clinical Pharmacology*, vol. 34, no. 2, pp. 160–172, 2020.
- [19] N. Baker, L. B. Boyette, and R. S. Tuan, "Characterization of bone marrow-derived mesenchymal stem cells in aging," *Bone*, vol. 70, pp. 37–47, 2015.
- [20] S. Yi, G. Han, Y. Shang et al., "Microbubble-mediated ultrasound promotes accumulation of bone marrow mesenchymal stem cell to the prostate for treating chronic bacterial prostatitis in rats," *Scientific Reports*, vol. 6, no. 1, Article ID 19745, 2016.
- [21] P. Tyagi, S. S. Motley, M. Kashyap et al., "Urine chemokines indicate pathogenic association of obesity with BPH/LUTS," *International Urology and Nephrology*, vol. 47, no. 7, pp. 1051–1058, 2015.
- [22] G. Paulis, "Inflammatory mechanisms and oxidative stress in prostatitis: the possible role of antioxidant therapy," *Research and Reports in Urology*, vol. 10, pp. 75–87, 2018.
- [23] F. F. Pasqualotto, R. K. Sharma, J. M. Potts, D. R. Nelson, A. J. Thomas, and A. Agarwal, "Seminal oxidative stress in patients with chronic prostatitis," *Urology*, vol. 55, no. 6, pp. 881–885, 2000.
- [24] J.-F. Zhou, W.-Q. Xiao, Y.-C. Zheng, J. Dong, and S.-M. Zhang, "Increased oxidative stress and oxidative damage associated with chronic bacterial prostatitis," *Asian Journal of Andrology*, vol. 8, no. 3, pp. 317–323, 2006.
- [25] S. Regmi, S. Pathak, J. O. Kim, C. S. Yong, and J.-H. Jeong, "Mesenchymal stem cell therapy for the treatment of inflammatory diseases: challenges, opportunities, and future perspectives," *European Journal of Cell Biology*, vol. 98, no. 5–8, Article ID 151041, 2019.
- [26] B. Zhang, R. Liu, D. Shi et al., "Mesenchymal stem cells induce mature dendritic cells into a novel Jagged-2-dependent regulatory dendritic cell population," *Blood*, vol. 113, no. 1, pp. 46–57, 2009.
- [27] S. Glennie, I. Soeiro, P. J. Dyson, E. W.-F. Lam, and F. Dazzi, "Bone marrow mesenchymal stem cells induce division arrest anergy of activated T cells," *Blood*, vol. 105, no. 7, pp. 2821–2827, 2005.
- [28] G. Ren, J. Su, L. Zhang et al., "Species variation in the mechanisms of mesenchymal stem cell-mediated immunosuppression," *Stem Cells*, vol. 27, no. 8, pp. 1954–1962, 2009.
- [29] K. Nemeth, A. Keane-Myers, J. M. Brown et al., "Bone marrow stromal cells use TGF- $\beta$  to suppress allergic responses in a mouse model of ragweed-induced asthma," *Proceedings of the National Academy of Sciences*, vol. 107, no. 12, pp. 5652–5657, 2010.
- [30] A. Krasnodembskaya, Y. Song, X. Fang et al., "Antibacterial effect of human mesenchymal stem cells is mediated in part from secretion of the antimicrobial peptide LL-37," *Stem Cells*, vol. 28, no. 12, pp. 2229–2238, 2010.
- [31] Y. Shang, D. Cui, and S. Yi, "Opening tight junctions may be key to opening the blood-prostate barrier," *Medical Science Monitor: International Medical Journal of Experimental and Clinical Research*, vol. 20, pp. 2504–2507, 2014.
- [32] L. Yin, Y. Tang, A. Pan, L. Yang, X. Zhu, and Y. Liu, "The application of IL-10 and TNF- $\alpha$  in expressed prostatic secretions and prostatic exosomal protein in urine in the diagnosis of patients with chronic prostatitis," *Medicine*, vol. 98, no. 33, Article ID e16848, 2019.
- [33] B. Debelec-Butuner, C. Alapinar, L. Varisli et al., "Inflammation-mediated abrogation of androgen signaling: an in vitro model of prostate cell inflammation," *Molecular Carcinogenesis*, vol. 53, no. 2, pp. 85–97, 2014.
- [34] R. B. Nadler, A. E. Koch, E. A. Calhoun et al., "IL-1 $\beta$  and TNF- $\alpha$  IN prostatic secretions are indicators IN the evaluation OF men with chronic prostatitis," *The Journal of Urology*, vol. 164, no. 1, pp. 214–218, 2000.
- [35] G. Penna, N. Mondaini, S. Amuchastegui et al., "Seminal plasma cytokines and chemokines in prostate inflammation: interleukin 8 as a predictive biomarker in chronic prostatitis/chronic pelvic pain syndrome and benign prostatic hyperplasia," *European Urology*, vol. 51, no. 2, pp. 524–533, 2007.

- [36] X. T. Huang, W. Liu, Y. Zhou et al., "Dihydroartemisinin attenuates lipopolysaccharide-induced acute lung injury in mice by suppressing NF- $\kappa$ B signaling in an Nrf2-dependent manner," *International Journal of Molecular Medicine*, vol. 44, pp. 2213–2222, 2019.
- [37] R. Liang, W. Chen, H. Fan, X. Chen, J. Zhang, and J.-S. Zhu, "Dihydroartemisinin prevents dextran sodium sulphate-induced colitis through inhibition of the activation of NLRP3 inflammasome and p38 MAPK signaling," *International Immunopharmacology*, vol. 88, Article ID 106949, 2020.
- [38] M. Fan, Y. Li, C. Yao, X. Liu, X. Liu, and J. Liu, "Dihydroartemisinin derivative DC32 attenuates collagen-induced arthritis in mice by restoring the Treg/Th17 balance and inhibiting synovitis through down-regulation of IL-6," *International Immunopharmacology*, vol. 65, pp. 233–243, 2018.
- [39] J. M. Potts and F. F. Pasqualotto, "Seminal oxidative stress in patients with chronic prostatitis," *Andrologia*, vol. 35, no. 5, pp. 304–308, 2003.
- [40] A. U. Ihsan, F. U. Khan, P. Khongorzul et al., "Role of oxidative stress in pathology of chronic prostatitis/chronic pelvic pain syndrome and male infertility and antioxidants function in ameliorating oxidative stress," *Biomedicine & Pharmacotherapy*, vol. 106, pp. 714–723, 2018.
- [41] Q. Zhao, F. Yang, L. Meng et al., "Lycopene attenuates chronic prostatitis/chronic pelvic pain syndrome by inhibiting oxidative stress and inflammation via the interaction of NF- $\kappa$ B, MAPKs, and Nrf2 signaling pathways in rats," *Andrology*, vol. 8, no. 3, pp. 747–755, 2020.
- [42] D.-X. Yang, J. Qiu, H.-H. Zhou et al., "Dihydroartemisinin alleviates oxidative stress in bleomycin-induced pulmonary fibrosis," *Life Sciences*, vol. 205, pp. 176–183, 2018.
- [43] A. Yoshimura, Y. Wakabayashi, and T. Mori, "Cellular and molecular basis for the regulation of inflammation by TGF- $\beta$ ," *Journal of Biochemistry*, vol. 147, no. 6, pp. 781–792, 2010.
- [44] M. M. Said, S. S. Azab, N. M. Saeed, and E. El-Demerdash, "Antifibrotic mechanism of pinocembrin: impact on oxidative stress, inflammation and TGF- $\beta$ /smad inhibition in rats," *Annals of Hepatology*, vol. 17, no. 2, pp. 307–317, 2018.
- [45] H. B. Rezaei, D. Kamato, G. Ansari, N. Osman, and P. J. Little, "Cell biology of Smad2/3 linker region phosphorylation in vascular smooth muscle," *Clinical and Experimental Pharmacology and Physiology*, vol. 39, no. 8, pp. 661–667, 2012.
- [46] H. Y. Lan, "Diverse roles of TGF- $\beta$ /smads in renal fibrosis and inflammation," *International Journal of Biological Sciences*, vol. 7, no. 7, pp. 1056–1067, 2011.
- [47] M. Gao, J. Zheng, C. Zheng, Z. Huang, and Q. Huang, "Theacrine alleviates chronic inflammation by enhancing TGF- $\beta$ -mediated shifts via TGF- $\beta$ /SMAD pathway in Freund's incomplete adjuvant-induced rats," *Biochemical and Biophysical Research Communications*, vol. 522, no. 3, pp. 743–748, 2020.